Oncogene (1999) 18, 2607–2615

http://www.stockton-press.co.uk/onc

Characterization of a naturally occurring ErbB4 isoform that does not bind or activate phosphatidyl inositol 3-kinase

Klaus Elenius[1,2], Caroline J Choi[1], Subroto Paul[1], Eric Santiestevan[1], Eiichiro Nishi[1] and Michael Klagsbrun*[,1]

[1]*Departments of Surgery and Pathology, Children's Hospital and Harvard Medical School, Boston, MA 02115, USA;* [2]*Medicity Research Laboratories, University of Turku, 20520 Turku, Finland*

Receptor tyrosine kinases regulate cell behavior by activating specific signal transduction cascades. Epidermal growth factor (EGF) receptor tyrosine kinases include ErbB1, ErbB2, ErbB3 and ErbB4. ErbB4 is a tyrosine kinase receptor that binds neuregulins (NRG) and several other EGF family members. Reverse transcriptase polymerase chain reaction (RT–PCR) analysis identified two isoforms of ErbB4 that differed in their cytoplasmic domain sequences. Specifically, RT–PCR using primers flanking the putative phosphatidyl inositol 3-kinase (PI3-K) binding site of ErbB4 generated two specific bands when human and mouse heart and kidney tissues were analysed. Cloning and sequencing of these RT–PCR products revealed that one of the ErbB4 isoforms (ErbB4 CYT-2) lacked a 16 amino acid sequence including a putative PI3-K binding site, that was present in the other isoform (ErbB4 CYT-1). RT–PCR analysis of mouse tissues suggested that the expression of ErbB4 CYT-1 and ErbB4 CYT-2 was tissue-specific. Heart, breast and abdominal aorta expressed predominantly ErbB4 CYT-1 whereas neural tissues and kidney expressed predominantly ErbB4 CYT-2. To ascertain whether the absence of the putative PI3-K binding site in ErbB4 CYT-2 also resulted in the loss of PI3-K activity, NIH3T3 cell lines overexpressing ErbB4 CYT-1 or ErbB4 CYT-2 were produced. NRG-1 bound to and stimulated equivalent tyrosine phosphorylation of both isoforms. However, unlike ErbB4 CYT-1, the ErbB4 CYT-2 isoform was unable to bind the p85 subunit of PI3-K and to stimulate PI3-K activity in these cells. Furthermore, tyrosine phosphorylation of p85 or association of PI3-K activity with phosphotyrosine was not induced in NRG-1 treated cells expressing ErbB4 CYT-2, indicating that this isoform was incapable of activating PI3-K even indirectly. It was concluded that a novel naturally occurring ErbB4 isoform exists with a deletion of the cytoplasmic domain sequence required for the activation of the PI3-K intracellular signal transduction pathway and that this is the only PI3-K binding site in ErbB4.

Keywords: alternative splicing; chemotaxis; EGF receptor; survival

Introduction

The coordinated proliferation, survival, differentiation and chemotaxis of cells in developing tissues is controlled by soluble paracrine factors, many of which interact with receptor tyrosine kinases (RTK). Binding of a ligand to the extracellular domain of an RTK initiates receptor dimerization and autophosphorylation by the intrinsic tyrosine kinase residing in the cytoplasmic part of the RTK. The phosphorylated tyrosine residues, when represented in the correct context, serve as specific binding sites for intracellular signal transduction molecules, such as Grb2, Shc, GTPase activating protein (GAP), phospholipase C-γ (PLC-γ) and phosphatidyl inositol 3-kinase (PI3-K) (Schlessinger and Ullrich, 1992; Songyang *et al*., 1993). The quality, intensity and duration of the activated signals then determine which specific cellular responses are the outcome of RTK stimulation.

Epidermal growth factor receptor (EGFR)-like receptors constitute a subfamily of RTKs that currently includes four members: ErbB1 (HER1, EGFR), ErbB2 (HER2, c-Neu), ErbB3 (HER3) and ErbB4 (HER4) (Ullrich *et al*., 1984; Yamamoto *et al*., 1986; Kraus *et al*., 1989; Plowman *et al*., 1993). An important role for these receptors in regulating cell behavior during normal development has been demonstrated by generating null mice with targeted ErbB receptors. ErbB1 null mice have strain-dependent defects in the inner cell mass, placenta, brain and epithelial structures (Miettinen *et al*., 1995; Sibilia and Wagner, 1995; Threadgill *et al*., 1995; Sibilia *et al*., 1998). ErbB2 and ErbB4 null mice die 10–11 days after fertilization with defects in heart and brain (Gassmann *et al*., 1995; Lee *et al*., 1995). ErbB3 null mice lack Schwann cells and die with severe neuropathies (Riethmacher *et al*., 1997).

Receptors of the EGFR-like subfamily of RTKs interact with EGF-like ligands. ErbB1 is the receptor for EGF, transforming growth factor-α (TGF-α), amphiregulin (AR), heparin-binding EGF-like growth factor (HB-EGF), betacellulin (BTC) and epiregulin (ER) (Shoyab *et al*., 1989; Carpenter and Wahl, 1991; Higashiyama *et al*., 1991; Shing *et al*., 1993; Toyoda *et al*., 1995). ErbB2 is an orphan receptor but is activated in heterodimeric combinations with the other ErbBs (Wada *et al*., 1990; Hynes and Stern, 1994; Karunagaran *et al*., 1996). ErbB3 and ErbB4 are receptors for neuregulins, a gene family that includes three members (NRG-1, NRG-2 and NRG-3), each containing several alternatively spliced forms (Holmes *et al*., 1992; Wen *et al*., 1992; Falls *et al*., 1993; Marchionni *et al*., 1993; Carraway *et al*., 1997; Chang *et al*., 1997; Higashiyama *et al*., 1997; Zhang *et al*., 1997). Recent studies have indicated that ErbB4 can also interact with three other EGF-like growth factors, HB-EGF, BTC and ER, that were initially characterized as ErbB1 ligands (Riese *et*

*Correspondence: M Klagsbrun
Received 11 August 1997; revised 14 December 1998; accepted 14 December 1998

al., 1996; Elenius *et al*., 1997b; Komurasaki *et al*., 1997).

ErbB4 is the most recently characterized member of the ErbB family (Plowman *et al*., 1993). It is a 180 kD transmembrane glycoprotein with the highest expression levels in heart, kidney and in neuronal tissues (Plowman *et al*., 1993; Elenius *et al*., 1997a). ErbB4 is expressed in high levels also in some mammary adenocarcinoma, neuroblastoma and pancreatic carcinoma cell lines (Plowman *et al*., 1993) and its overexpression along with that of ErbB2 in human medulloblastoma is an independent prognostic factor for patient survival (Gilbertson *et al*., 1997). Activation of ErbB4 by its ligands leads to interaction of specific signal transduction molecules, such as PI3-K and Shc, with phosphorylated tyrosines in the cytoplasmic tail of ErbB4, eventually resulting in cellular proliferation, chemotaxis, differentiation and survival (Plowman *et al*., 1993; Culouscou *et al*., 1995; Dong *et al*., 1995; Cohen *et al*., 1996; Elenius *et al*., 1997b).

In a previous study we demonstrated the existence of two naturally occurring ErbB4 isoforms (ErbB4 JM-a and ErbB4 JM-b) that differed structurally in their juxtamembrane domain sequence and functionally in their susceptibility to phorbol ester-stimulated proteolysis (Elenius *et al*., 1997a). We now report the identification of another novel naturally occurring ErbB4 isoform, one that lacks amino acids 1046–1061 when compared to the human ErbB4 sequence described originally (Plowman *et al*., 1993). These 16 amino acids reside in the cytoplasmic tail of ErbB4 and include a Tyr-X-X-Met consensus sequence (residues 1056–1059 in human ErbB4) that constitutes a consensus binding site for the p85 subunit of PI3-K (Songyang *et al*., 1993). Furthermore, we demonstrate in cell culture, that the isoform lacking the p85 consensus binding site is functional in that it binds NRG-1, is tyrosine phosphorylated in response to NRG-1, but has lost its capacity to bind p85 or to stimulate PI3-K activity. We have named the novel isoform lacking the 16 amino acids, ErbB4 CYT-2, and the isoform corresponding to the original ErbB4 sequence (Plowman *et al*., 1993), ErbB4 CYT-1. ErbB4 CYT-2 is expressed predominantly in neural tissues and kidney, while ErbB4 CYT-1 is expressed predominantly in heart and breast. Taken together, these findings demonstrate the existence *in vivo* of two isoforms of ErbB4, which differ in their ability to activate specifically the PI3-K signal transduction pathway.

Results

Identification and sequencing of ErbB4 cytoplasmic isoforms

In order to analyse human and mouse ErbB4 mRNAs in various tissues, primers were designed corresponding to a cytoplasmic sequence of human ErbB4 cDNA (Plowman *et al*., 1993) and to a homologous region in the partial mouse ErbB4 cDNA sequence (Moscoso *et al*., 1995). These primers were used for RT–PCR analysis of total RNA isolated from human and mouse tissues. RT–PCR analysis of both human and mouse heart and kidney tissues produced, however, three distinct bands each, rather than the one that had been expected (Figure 1). In order to characterize the RT–PCR products more fully, they were cloned into a pCR3.1 vector. The identities of the bands derived from human kidney and mouse heart were determined by sequencing the inserts (Figure 2a). The sequence of the 294 bp product (Figure 1, lane 2, middle band) of human kidney was identical to a cytoplasmic one in the original human ErbB4 sequence (Plowman *et al*., 1993). The smaller 246 bp PCR product (Figure 1, lane 2, lower band) differed from the original human ErbB4 sequence in having an in-frame deletion of 48 nucleotides encoding 16 amino acids at positions 1046–1061 in the cytoplasmic domain. The 252 bp PCR product (Figure 1, lane 3, middle band), cloned from mouse heart was homologous to the 294 bp human product. The 204 bp PCR product from mouse heart (Figure 1, lane 3, lower band) was identical to a partial mouse ErbB4 sequence (Moscoso *et al*., 1995) and differed from the mouse 252 bp PCR product by having a deletion of 48 nucleotides encoding 16 amino acids corresponding to positions 1046–1061 in the human ErbB4 sequence. The largest bands generated by RT–PCR (human approximately 360 bp and mouse approximately 310 bp) were eventually found to be artifacts produced as a result of annealing of the

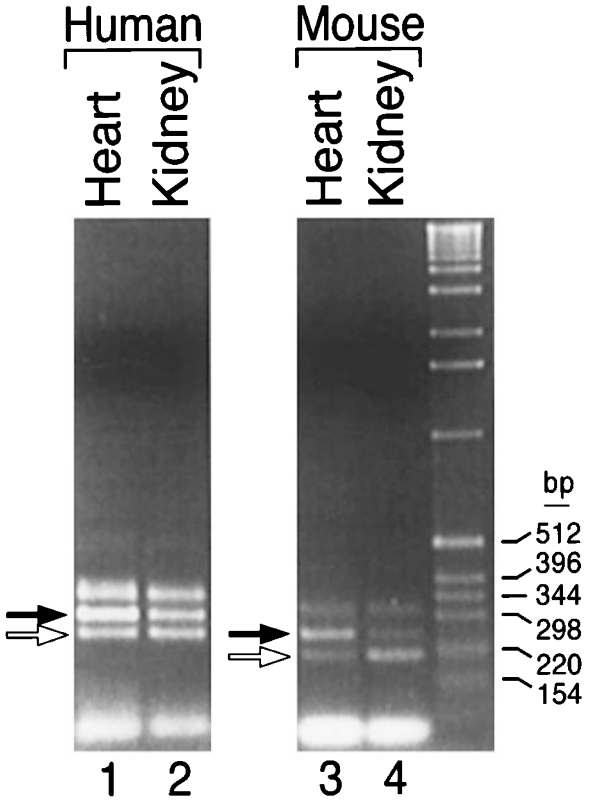

Figure 1 RT–PCR analysis with ErbB4-specific primers designed corresponding to sequences flanking the PI3-K binding site. Total RNA was isolated from human heart (lane 1), human kidney (lane 2), mouse heart (lane 3) and mouse kidney (lane 4) and subjected to RT–PCR analysis. The PCR products were separated on a 2% agarose gel and visualized under ultraviolet light after staining with ethidium bromide. A 1 Kb ladder was used as a size marker. The arrows point to the two bands that were cloned, solid arrows for the middle bands and open arrows for the lower bands

two smaller products to each other during the PCR cycling (data not shown).

These results demonstrated that two isoforms with or without a 16 amino acid deletion within the cytoplasmic tail of the ErbB4 receptor exist in both human and mouse tissues. The isoform identical to the published human sequence was named ErbB4 CYT-1, and the isoform with the 16 amino acid deletion was named ErbB4 CYT-2, based on the deletion being within the cytoplasmic domain (Figure 2b) and the order of their discovery. The 16 amino acid sequence found in ErbB4 CYT-1 and lacking in ErbB4 CYT-2 contained a Tyr-Thr-Pro-Met sequence, previously suggested to serve as the site for the binding of p85 to the activated ErbB4 (Figure 2b) (Cohen *et al*., 1996).

The expression of ErbB4 cytoplasmic isoforms in mouse tissues is regulated in a tissue-specific manner

A series of mouse tissues were analysed for ErbB4 cytoplasmic isoform expression (Figure 3). RNA was purified from over 20 mouse tissues and analysed by RT–PCR using primers flanking the differential cytoplasmic region. Whereas some tissues such as heart, breast and abdominal aorta (Figure 3, top panel, lanes 1, 2 and 20, respectively) expressed predominantly ErbB4 CYT-1, others, in particular neural tissues such as cerebellum, cerebral cortex, spinal cord and medulla oblongata (Figure 3, top panel, lanes 11, 12, 15 and 16, respectively) expressed predominantly ErbB4 CYT-2. Some tissues, including

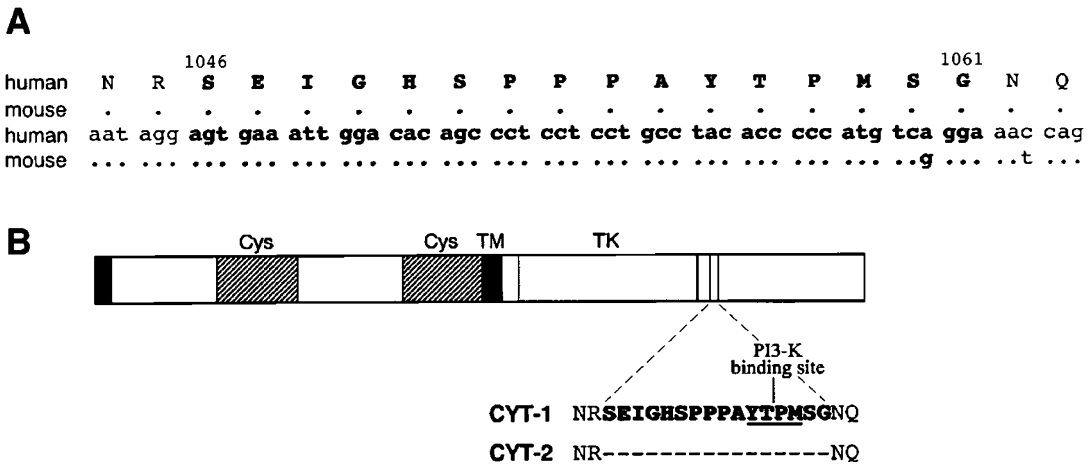

Figure 2 Nucleotide and deduced amino acid sequences of the ErbB4 cytoplasmic isoforms. (**a**) The RT–PCR products obtained using primers flanking the PI3-K binding site derived from the human kidney and mouse heart samples in Figure 1 (two lower bands in each species) were cloned into a pCR3.1 vector and the inserts were sequenced. The 48 nucleotide (16 amino acid) insert including the PI3-K binding site present in ErbB4 CYT-1, but not in ErbB4 CYT-2, is shown in boldface, and two amino acids (NR and NQ) flanking either end are shown in plain font to put the deletion into context. The numbers 1046 and 1061 refer to the positions within the published human ErbB4 sequence (Plowman *et al*., 1993) of the first (S) and last amino acid residues (G) which are missing in CYT-2. The dots within the mouse sequences indicate amino acids and nucleotides identical to the human sequences. (**b**) A schematic diagram of ErbB4 CYT-1 and ErbB4 CYT-2 isoforms. The amino acid sequence present in the CYT-1 isoform, but not in the CYT-2 isoform, is shown in boldface. The horizontal dashes within the CYT-2 sequence indicate the sites of the missing amino acids when compared to the CYT-1 sequence. The binding sequence for the p85 subunit of PI3-K, Tyr-Thr-Pro-Met, is underlined. Cys, cysteine rich domain; TM, transmembrane domain; TK, tyrosine kinase domain

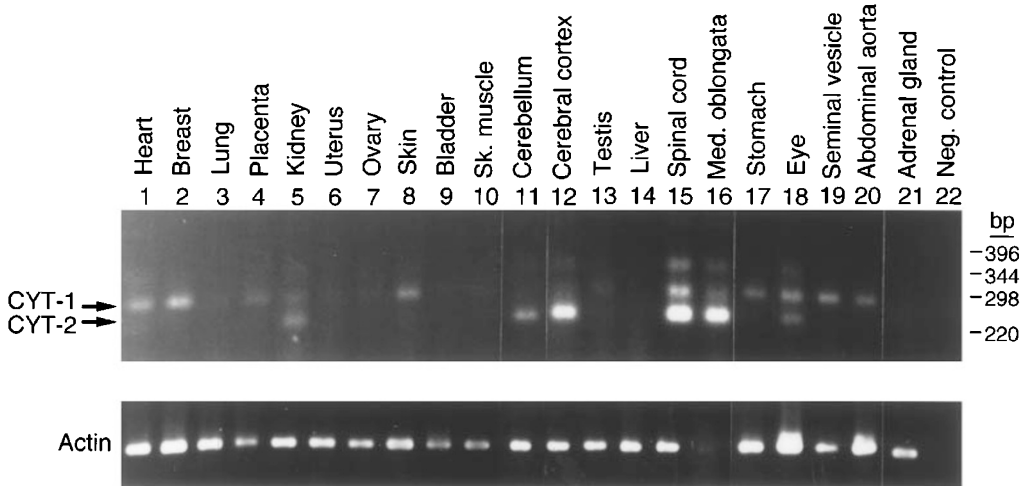

Figure 3 RT–PCR analysis of the distribution of ErbB4 CYT isoforms in mouse tissues. Total RNA was isolated and subjected to RT–PCR analysis with mouse ErbB4-specific primers designed corresponding to cDNA sequences flanking the PI3-K binding site. As an internal standard, all the templates were also analysed by PCR using primers specific for mouse β-actin (bottom panel). Lane 22 (negative control) shows a PCR reaction in the absence of templates

lung, bladder and liver (Figure 3, top panel, lanes 3, 9 and 14) expressed very little, if any, of either one of the isoforms. To generate an internal standard for the RT–PCR reaction, the same reverse transcriptase products used for ErbB4-specific PCR were analysed by PCR using primers specific for mouse β-actin. A single band of the expected size (450 bp) was detected in all the samples (Figure 3, bottom panel, lanes 1–21). No product was detected when PCR was performed with either set of primers in the absence of a cDNA template (Figure 3, both panels, lane 22). These studies indicated that the expression of the two cytoplasmic isoforms was regulated in a tissue-specific manner.

Both ErbB4 cytoplasmic isoforms are functional receptors

ErbB4 CYT-2 lacks the Tyr-X-X-Met consensus sequence (residues 1056–1059) that constitutes a consensus binding site for the p85 subunit of PI3-K (Songyang *et al*., 1993). In order to demonstrate that this isoform is functional but has lost its ability to bind p85 and to stimulate PI3-K activity, stable NIH3T3 cell transfectants expressing either ErbB4 CYT-1 or ErbB4 CYT-2 were generated. A previously described expression vector (cH4M2 JM-b) was used to express the ErbB4 CYT-1 isoform (Elenius *et al*., 1997a). To construct an ErbB4 CYT-2 expression vector, RT–PCR products from human kidney were generated with primers flanking the alternative cytoplasmic region. A 592 bp *Xho*I/*Nsi*I fragment of a RT–PCR product matching the size of the CYT-2 form was cloned into the cH4M2 JM-b expression vector to replace the corresponding 640 bp *Xho*I/*Nsi*I fragment. This vector was designated cH4M2 JM-b CYT-2 and its sequence was confirmed. The two expression vectors were introduced into NIH3T3 clone seven cells, which are devoid of detectable levels of any endogenous ErbB receptor expression (Zhang *et al*., 1996) and which have been previously used to analyse the function of ErbB4 juxtamembrane isoforms (Elenius *et al*., 1997a). Several clones expressing one or the other of the ErbB4 cytoplasmic isoforms were obtained. The clones expressing the JM-b CYT-1 isoform of ErbB4 were designated with the prefix b1 and the clones expressing the JM-b CYT-2 isoform with the prefix b2. Control clones transfected with a neomycin resistance gene were designated with the prefix neo. ErbB4 protein synthesis was analysed by immunoprecipitation and Western blotting with anti-ErbB4 antibodies (Figure 4). No ErbB4 protein was detected in clones transfected with the vector encoding the neomycin resistance gene alone (Figure 4, lane 1). Two clones (b1.42 and b1.amg) expressed ErbB4 CYT-1 (Figure 4, lanes 2 and 3) and two clones (b2.11 and b2.15) expressed ErbB4 CYT-2 (Figure 4, lanes 4 and 5). The expression levels of ErbB4 proteins by these cell lines were fairly equivalent.

To determine whether both types of cytoplasmic isoforms were expressed at the cell surfaces and were capable of binding soluble ErbB4 ligands, cross-linking analysis with radioiodinated NRG-1 (^{125}I-NRG-1) was performed. Cross-linking of ^{125}I-NRG-1 to both clones expressing ErbB4 CYT-1 and to both clones expressing ErbB4 CYT-2 resulted in the formation of a 190 kDa complex, as expected for the covalent binding of a single 7 kD NRG-1 molecule to a single 180 kD ErbB4 molecule (Figure 5, lanes 2–5). No cross-linked complex was observed when ^{125}I-NRG-1 was cross-linked to control cells transfected with the neomycin resistance gene alone and not expressing ErbB4 (Figure 5, lane 1).

To examine whether the intrinsic tyrosine kinase activity of both ErbB4 isoforms were activated in response to ligand binding, two clones each of cells expressing ErbB4 CYT-1 and ErbB4 CYT-2 were

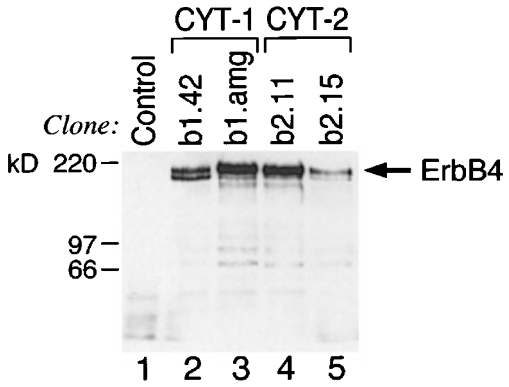

Figure 4 ErbB4 protein levels in cells expressing ErbB4 cytoplasmic isoforms. Lysates of a control clone transfected with a plasmid encoding a neomycin resistance gene alone (lane 1), of two independent clones (b1.42 and b1.amg) co-transfected with a neomycin resistance gene plasmid and an expression plasmid for ErbB4 CYT-1 (lanes 2 and 3), and of two independent clones (b2.11 and b2.15) cotransfected with a neomycin resistance gene plasmid and an expression plasmid for ErbB4 CYT-2 (lanes 4 and 5) were prepared. Protein levels in cell lysates were analysed by a combination of immunoprecipitation and Western blotting, using anti-ErbB4-specific antibodies. The samples were separated on a 6% SDS–PAGE and visualized by ECL. An arrow points to the position of ErbB4

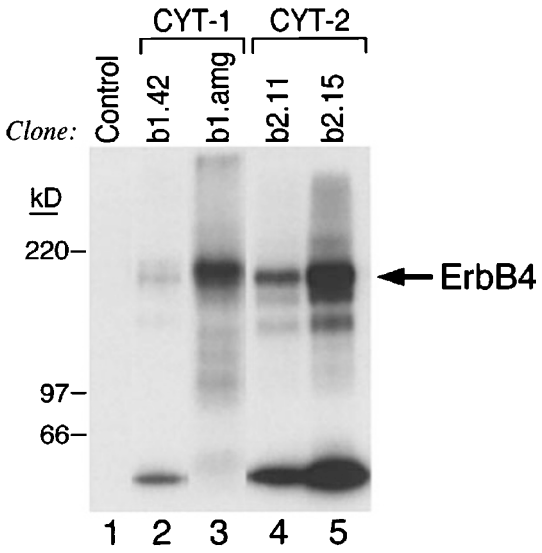

Figure 5 Cross-linking of ^{125}I-NRG-1 to cells expressing ErbB4 cytoplasmic isoforms. Control cells (lane 1), cells expressing ErbB4 CYT-1 (lanes 2 and 3) and cells expressing ErbB4 CYT-2 (lanes 4 and 5) were cross-linked with DSS in the presence of ^{125}I-NRG-1. The cells were lysed and the cross-linked complexes were separated on a 6% SDS–PAGE and visualized by autoradiography. An arrow points to the 190 kD ^{125}I-NRG-1/ErbB4 complex

stimulated with or without NRG-1 and analysed for ErbB4 tyrosine phosphorylation. Both ErbB4 cytoplasmic isoforms were activated to a similar extent by NRG-1 (Figure 6, lanes 3–10). No ErbB4 phosphorylation was observed in the control cells transfected with the neomycin resistance gene alone (Figure 6, lanes 1 and 2). Taken together, these two experiments indicate that both ErbB4 cytoplasmic isoforms are functional cell surface receptors capable of binding an ErbB ligand and activating tyrosine phosphorylation.

ErbB4 CYT-2 does not bind to or activate PI3-K

The lack of a PI3-K consensus binding site in the cytoplasmic domain of ErbB4 CYT-2 suggests that the interaction of this isoform with PI3-K would be impaired. Accordingly, the association of the two ErbB4 cytoplasmic isoforms with PI3-K was assessed by co-precipitation experiments. Control cells expressing neomycin resistance gene alone and cells expressing ErbB4 CYT-1 or ErbB4 CYT-2 were treated with or without NRG-1, their lysates were immunoprecipitated with an antibody directed against the p85 subunit or PI3-K and the immunoprecipitated material was analysed by Western blotting with an antibody directed against ErbB4 (Figure 7a). When cells expressing ErbB4 CYT-1 were analysed, a 180 kD band immunoreactive with anti-ErbB4 was co-precipitated with anti-p85 (Figure 7a, lane 3). The intensity of this band increased in response to stimulation of the cells with NRG-1 (Figure 7a, lane 4), consistent with previous reports that NRG-1 up-regulates the association of p85 with ErbB4 (Cohen *et al*., 1996; Elenius *et al*., 1997b). On the other hand, no association of p85 with ErbB4 was detected in cells expressing ErbB4 CYT-2 (Figure 7a, lanes 5 and 6) or in neo control cells not expressing ErbB4 (Figure 7a, lanes 1 and 2) either with or without NRG-1 stimulation. These results demonstrate that the 16 amino acids missing in the cytoplasmic domain of ErbB4 CYT-2 include the major binding site in ErbB4 for PI3-K and rule out the possibility that there may be other direct PI3-K binding sites elsewhere in the cytoplasmic domain.

To analyse PI3-K activity, control cells and cells expressing ErbB4 CYT-1 or ErbB4 CYT-2 were analysed by anti-ErbB4 immunoprecipitation followed by a PI3-K *in vitro* kinase assay and thin layer chromatography (TLC) (Figure 7b). Cells expresing ErbB4 CYT-1 demonstrated NRG-1-induced association of PI3-K activity with ErbB4 as measured by formation of PI^{32}P (Figure 7b, lanes 3 and 4) whereas no ErbB4-associated PI3-K activity was detected in cells expressing ErbB4 CYT-2 (Figure 7b, lanes 5 and 6) or in neo controls not expressing ErbB4 (Figure 7b, lanes 1 and 2). These results are consistent with the immunoprecipitation data shown in Figure 7a. To obtain standards for the migration of the phosphorylated phosphatidyl inositol substrate on the TLC plate, PI3-K activity was immunoprecipitated directly from NRG-1-stimulated ErbB4 CYT-1 and ErbB4 CYT-2 cell clones respectively with an anti-p85 antibody (Figure 7B, lanes 7 and 8).

We have demonstrated that ErbB4 CYT-2 cannot directly bind PI3-K. This isoform could, however, activate PI3-K indirectly, for example via an adapter molecule such as Grb-2-associated binder-1 (Gab-1)

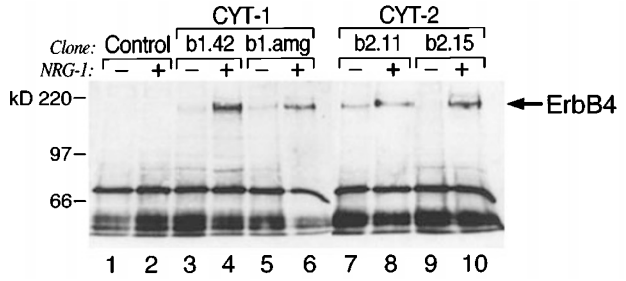

Figure 6 Tyrosine phosphorylation of ErbB4 cytoplasmic isoforms. Control cells (lanes 1 and 2), cells expressing ErbB4 CYT-1 (lanes 3–6) or cells expressing ErbB4 CYT-2 (lanes 7–10) were stimulated without (lanes 1, 3, 5, 7 and 9) or with (lanes 2, 4, 6, 8 and 10) 100 ng/ml NRG-1. The cells were lysed and the lysates were immunoprecipitated with an anti-ErbB4 antibody. The precipitated material was separated on a 6% SDS–PAGE and the tyrosine phosphorylated proteins were visualized by Western blotting with an antiphosphotyrosine antibody followed by ECL. An arrow points to the position of ErbB4

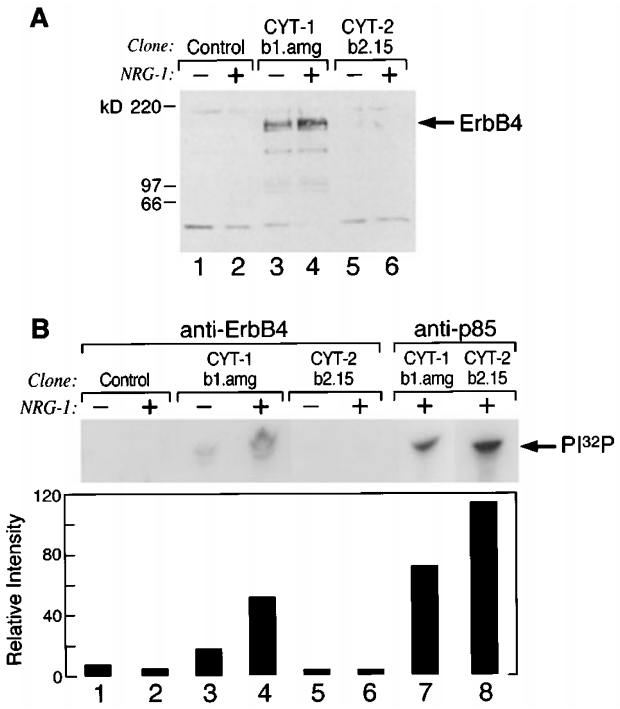

Figure 7 Association of PI3-K with ErbB4 cytoplasmic isoforms. (**a**) Co-precipitation of ErbB4 with p85. Control cells (lanes 1 and 2), cells expressing ErbB4 CYT-1 (b1.amg, lanes 3 and 4) or cells expressing ErbB4 CYT-2 (b2.15, lanes 5 and 6) were stimulated without (lanes 1, 3 and 5) or with (lanes 2, 4 and 6) 100 ng/ml NRG-1. Cells were lysed and the lysates were immunoprecipitated with an anti-p85 antibody. The precipitated material was separated on a 6% SDS–PAGE and analysed by Western blotting with an anti-ErbB4 antibody followed by ECL. An arrow points to the position of ErbB4. (**b**) Association of PI3-K activity with ErbB4. Control cells (lanes 1 and 2), cells expressing ErbB4 CYT-1 (lanes 3, 4 and 7) or cells expressing ErbB4 CYT-2 (lanes 5, 6 and 8) were stimulated without (lanes 1, 3 and 5) or with (lanes 2, 4 and 6–8) NRG-1. Cells were lysed and lysates were immunoprecipitated with an anti-ErbB4 antibody (lanes 1–6) or anti-p85 antibody (lanes 7 and 8). The precipitated material was analysed for PI3-K activity *in vitro* by visualizing the incorporation of ^{32}P into PI^{32}P with TLC and autoradiography. The intensity of PI^{32}P signals was quantitated by densitometry using the NIH Image program. Both the TLC signals and densitometric results are shown. Similar results were obtained when the independent clones b1.42 and b2.11 were analysed

that links PI3-K to Grb-2 (Holgado-Madruga *et al*., 1996). To assess whether ErbB4 CYT-2 could activate PI3-K indirectly, tyrosine phosphorylation of the p85 subunit of PI3-K was analysed by immunoprecipitation with anti-p85 antibody followed by Western blot with anti-phosphotyrosine antibody (Figure 8a). Lysates of cells expressing ErbB4 CYT-1 contained specific tyrosine phosphorylated proteins of 85 kD and 180 kD, whose phosphorylation was induced by NRG-1 (Figure 8a, lanes 3 and 4). Re-blotting the membrane with anti-p85 and anti-ErbB4 antibodies demonstrated that these proteins were p85 and the co-precipitated 180 kD ErbB4 receptor, respectively (not shown). In contrast, no significant tyrosine phosphorylation of 85 kD or 180 kD bands was detected in cells expressing ErbB4 CYT-2 (Figure 8a, lanes 5 and 6) or neo control cells (Figure 8a, lanes 1 and 2). These results demonstrating that p85 was tyrosine phosphorylated in cells expressing ErbB4 CYT-1 but not in cells expressing ErbB4 CYT-2. Next a PI3-K *in vitro* kinase assay was performed after immunoprecipitation with an anti-phosphotyrosine antibody. Phosphorytosine-associated PI3-K activity was detected in cells expressing ErbB4 CYT-1 after stimulation with NRG-1 (Figure 8b, lanes 3 and 4) but no such activity was detected in cells expressing ErbB4 CYT-2 (Figure 8b, lanes 5 and 6) or in control cells (Figure 8b, lanes 1 and 2). $PI^{32}P$ standards were obtained by direct anti-p85 immunoprecipitation from NRG-1-stimulated ErbB4 CYT-1 and ErbB4 CYT-2 cell clones (Figure 8b, lanes 7 and 8). These results suggested that PI3-K was not activated even indirectly in cells expressing ErbB4 CYT-2.

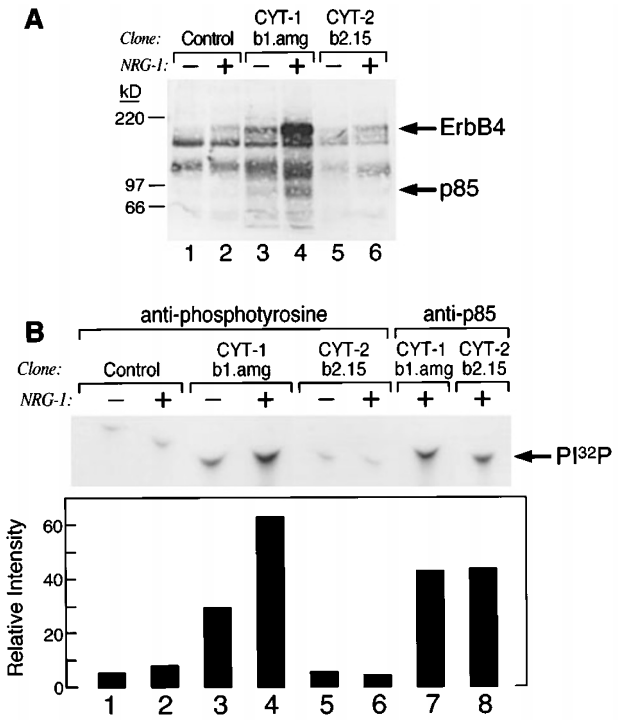

Figure 8 Activation of PI3-K by ErbB4 cytoplasmic isoforms. (**a**) Tyrosine phosphorylation of p85. Control cells (lanes 1 and 2), cells expressing ErbB4 CYT-1 (b1.amg, lanes 3 and 4) or cells expressing ErbB4 CYT-2 (b2.15, lanes 5 and 6) were stimulated without (lanes 1, 3 and 5) or with (lanes 2, 4 and 6) 100 ng/ml NRG-1. The cells were lysed and the lysates were immunoprecipitated with an anti-p85 antibody. The precipitated material was separated on a 6% SDS–PAGE and the tyrosine phosphorylated proteins were visualized by Western blotting with an antiphosphotyrosine antibody followed by ECL. Arrows point to positions of the 85 kD p85 band and the 180 kD ErbB4 band. (**b**) Association of PI3-K activity with phosphotyrosine. Control cells (lanes 1 and 2), cells expressing ErbB4 CYT-1 (lanes 3, 4 and 7) or cells expressing ErbB4 CYT-2 (lanes 5, 6 and 8) were stimulated without (lanes 1, 3 and 5) or with (lanes 2, 4 and 6–8) NRG-1. Cells were lysed and lysates were immunoprecipitated with an antiphosphotyrosine antibody (lanes 1–6) or anti-p85 antibody (lanes 7 and 8). The precipitated material was then analysed for PI-3-K activity *in vitro* by visualizing the incorporation of ^{32}P into $PI^{32}P$ with TLC and autoradiography. The intensity of $PI^{32}P$ signals was quantitated by densitometry using the NIH Image program. Both the TLC signals and densitometric results are shown. Similar results were obtained when the independent clones b1.42 and b2.11 were analysed

Discussion

This report presents evidence that the ErbB4 receptor exists *in vivo* in two isoforms, probably as a result of alternative splicing, that differ in whether or not they include a 16 amino acid stretch in the cytoplasmic domain that contains a consensus binding site for the p85 subunit of PI3-K. These isoforms, ErbB4 CYT-1, which includes the PI3-K binding domain, and ErbB4 CYT-2, which does not, were detected by RT–PCR analysis of human and mouse, heart and kidney tissue. Both isoforms were demonstrated to be functional NRG-1 receptors. When expressed in NIH3T3 cells, they bound NRG-1 to the cell surface and were tyrosine phosphorylated in response to NRG-1 stimulation. However, the isoforms differ in that cells expressing ErbB4 CYT-2 could not bind or activate PI3-K in a ligand-dependent manner. These results suggest strongly that Tyr_{1056} of human ErbB4, which is located in the 16 amino acid sequence lacking in ErbB4 CYT-2, is the only tyrosine residue within the cytoplasmic tail of ErbB4 that can interact with the p85 subunit of PI3-K. This result is consistent with the report that a synthetic peptide corresponding to residues 1054–1063 including a phosphorylated Tyr_{1056} inhibits the binding of PI3-K to ErbB4 (Cohen *et al*., 1996). There is the possibility, however, that the ErbB4 isoform lacking the PI3-K binding domain could activate PI3-K signaling indirectly via an adapter molecule or by ErbB receptor heterodimerization. For example, ErbB1 has been reported to activate PI3-K by indirect mechanisms, via the ErbB3 receptor (Soltoff *et al*., 1994), or the adapter molecules Cbl (Soltoff and Cantley, 1996) and Gab-1 (Holgado-Madruga *et al*., 1996). However, these considerations probably do not apply to the ErbB4 CYT-2 isoform since the cells lines used here do not express ErbB3 (Zhang *et al*., 1996) and Cbl has been shown to selectively bind to ErbB1 but not to ErbB4 (Levkowitz *et al*., 1996). Furthermore, we were able to rule out experimentally indirect PI3-K activation in cells expressing ErbB4 CYT-2 by demonstrating that NRG-1 stimulation could not induce tyrosine phosphorylation of p85, nor detectable phosphotyrosine-associated PI3-K activity in these cells. Taken together, our results suggest that ErbB4 CYT-2 is a functional receptor that responds to NRG-1 but it is a receptor that is unable to stimulate PI3-K activity in NIH3T3 cells either directly or indirectly due to lack of a p85 binding site.

An isoform that lacks the ability to activate PI3-K signaling might be functionally significant since signaling through the PI3-K pathway has been demonstrated to lead to numerous cellular responses, such as proliferation, survival, chemotaxis, actin rearrangements and changes in adhesion and protein trafficking (Toker and Cantley, 1997). In a previous study of ErbB4-mediated chemotaxis, we demonstrated that NRG-1 and HB-EGF stimulated chemotaxis of cells expressing ErbB4 in the absence of other EGFR-like receptors (Elenius *et al*., 1997b). Activation of ErbB4 by NRG-1 and HB-EGF stimulated a direct association of PI3-K activity with ErbB4. Nanomolar concentrations of wortmannin, a known inhibitor of PI3-K activity, were effective in abolishing the chemotactic response after stimulation with ErbB4 ligands (Elenius *et al*., 1997b). These results suggested a role for PI3-K activity in the signal transduction pathway leading from activated ErbB4 to chemotaxis. However, to date we have not been able to determine definitively whether the ErbB4 CYT-2 isoform is impaired or not in mediating chemotaxis via PI3-K. Another functional possibility is that cells expressing ErbB4 CYT-2 do not survive as well as do cells expressing ErbB4 CYT-1 in response to adverse conditions. PI3-K signaling has recently been implicated as having a central role in the pathway leading from an activated RTK to cellular survival (Yao and Cooper, 1995; Franke *et al*., 1997). NRG-1, a ligand that can activate ErbB4, promotes survival signaling in various cell types (Pinkas-Kramarski *et al*., 1994; Dong *et al*., 1995; Bermingham-McDonough *et al*., 1996; Canoll *et al*., 1996; Zhao *et al*., 1998). Our preliminary data suggest that NRG-1 promotes survival of serum-starved NIH3T3 cells expressing ErbB4 CYT-1 but not of cells expressing ErbB4 CYT-2.

ErbB4 isoforms differing in the presence of a PI3-K binding domain are not the only ones that exist. In a previous study, we found that there were ErbB4 isoforms that differed in the structure of the extracellular juxtamembrane domain, whereby 23 amino acids in one isoform were replaced by 13 other amino acids in the other isoform, suggesting alternative splicing of exons (Elenius *et al*., 1997a). These juxtamembrane isoforms were named ErbB4 JM-a and ErbB4 JM-b for the 23 amino acid form and the 13 amino acid form, respectively. Both ErbB4 JM-a and ErbB4 JM-b were equally activated by known ErbB4 ligands. However, ErbB4 JM-a was found to be susceptible to proteolytic cleavage of the receptor extracellular domain in response to treatment with phorbol ester, whereas ErbB4 JM-b was not (Elenius *et al*., 1997a). Given the existence of juxtamembrane and cytoplasmic isoform pairs, it appears that there are at least four possible ErbB4 isoforms in existence and possibly other ones as yet undiscovered.

Only one human ErbB4 gene has been identified (Zimonjic *et al*., 1995). Since the sequences of ErbB4 CYT-1 and ErbB4 CYT-2 flanking the alternative 16 amino acid insert were identical, it is most probable that these two isoforms are generated by alternative splicing of a single ErbB4 RNA precursor molecule. Differential expression of ErbB4 CYT-1 and ErbB4 CYT-2 by different mouse tissues suggested that this alternative splicing is regulated in a tissue-specific manner. Some tissues, such as heart and breast, express predominantly ErbB4 CYT-1, but several neural tissues, such as cerebellum, cerebral cortex, spinal cord and medulla oblongata express predominantly ErbB4 CYT-2. The significance of this distribution profile is unclear. However, the balance between survival and apoptosis in the developing nervous system and in the progression of neurodegenerative diseases, combined with the role of PI3-K signaling in mediating survival signaling in neural cells (Yao and Cooper, 1995; Franke *et al*., 1997), suggests a possible role for normal and PI3-K impaired ErbB4 isoforms in the nervous system. Recently, there was a report that ErbB4 isoforms with and without a PI3-K binding domain were expressed in normal breast and in breast tumor cell lines (Sawyer *et al*., 1998). However, no significant differential expression patterns were noticed between normal and malignant cells. Nevertheless, these and our results suggest that a thorough analysis of ErbB4 isoforms in normal tissue and malignant tumors is warranted in order to determine whether expression of these isoforms is biologically significant.

In summary, we have demonstrated that an isoform of ErbB4 exists *in vivo* that is functionally active in culture in terms of ligand binding and receptor activation, but that is not able to activate a specific downstream signal transduction molecule, PI3-K, either directly or indirectly. The existence of ErbB4 isoforms represents a novel mechanism for regulating a specific function of a receptor tyrosine kinase.

Materials and methods

RT–PCR and sequencing

Total RNA was isolated from the myocardium of the left ventricle of human heart, from human kidney and from various tissues obtained from 19–21 g Swiss Webster mice (Charles River Laboratories) by using RNAzol B reagent according to the manufacturer's instructions (Tel-Test, Inc.). Total RNA (2.5 μg) was subsequently reverse transcribed to cDNA with Superscript II enzyme according to the manufacturer's instructions (GIBCO–BRL) using random oligonucleotide primers (GIBCO–BRL). The cDNA was subjected to PCR analysis with primer pairs flanking the sequence encoding the p85 binding site in the cytoplasmic tail of ErbB4 or with primers specific for β-actin. Human ErbB4 cDNA was amplified with primers 5′-GAAGAGGATTTGGAAGATATGATG-3′ and 5′-ACAGCAGGAGTCATCAAAAATCTC-3′ (Plowman *et al*., 1993), mouse ErbB4 cDNA with primers 5′-GCTGAGGAATATTTGGTCCCCCAG-3′ and 5′-AAACATCTCAGCCGTTGCACCCTG-3′ (Moscoso *et al*., 1995), and mouse β-actin cDNA with primers 5′-CTACAATGAGCTGCGTGTGG-3′ and 5′-TAGCTCTTCTCCAGGGAGGA-3′ (Tokunaga *et al*., 1986), as previously described (Elenius *et al*., 1997a). The PCR reactions were carried out for 40 cycles with the annealing steps at 60°C. The PCR products were separated on a 2% agarose gel and visualized under ultraviolet light after staining with ethidium bromide. A 1 Kb DNA ladder (GIBCO–BRL) was used as a size marker. For sequencing, cytoplasmic ErbB4 RT–PCR amplicons from human kidney and mouse heart were cloned into a pCR3.1 vector using a TA Cloning Kit (Invitrogen). The inserts were sequenced using T7 or pCR3.1 reverse primers (Invitrogen) by chain termination sequencing using a Sequenase Version 2.0 DNA sequencing kit (USB).

Expression vectors and transfection

To generate stable cell lines expressing ErbB4 CYT-1 and ErbB4 CYT-2, the CYT-2 sequence was amplified by RT–PCR from human kidney and introduced into an ErbB4 CYT-1 expression vector, cH4M2 JM-b (Elenius *et al*., 1997a). To achieve this, ErbB4 cDNA was amplified with a primer pair 5′-AGTTTTCAAGGATGGCTCGAGACC-3′ and 5′-ACCATTGGATGCATTGTGATATTC-3′ specific for sequences flanking the alternative cytoplasmic region (Plowman *et al*., 1993). The RT–PCR products that were generated (665 bp and 617 bp) were cloned into the pCR3.1 vector using a TA Cloning Kit (Invitrogen). A 592 bp *Xho*I/*Nsi*I fragment of the smaller 617 bp insert (matching the size of the CYT-2 form) was then cloned into the cH4M2 JM-b expression vector to replace the corresponding 640 bp *Xho*I/*Nsi*I fragment. This procedure generated a cH4M2 JM-b CYT-2 expression plasmid that differed from the original cH4M2 JM-b CYT-1 expression plasmid only in the alternative cytoplasmic sequences. The sequences of the alternative domains of both expression vectors were confirmed by sequencing. Both cH4M2 JM-b CYT-1 and cH4M2 JM-b CYT-2 were separately cotransfected with a neomycin resistance gene encoding plasmid (pMAMneo; Clontech) into NIH3T3 clone seven cells (Zhang *et al*., 1996) using Lipofectin (GIBCO–BRL) according to the manufacturer's recommendations. Clones transfected with pMAMneo plasmid alone were generated and used as negative controls. Cells were subsequently cultured in DMEM supplemented with 10% fetal bovine serum, 1% glutamine/penicillin/streptomycin supplement (GPS: Irvine Scientific), 4.5 g/l glucose and 500 μg/ml G418 (Geneticin; GIBCO–BRL). G418-resistant clones were screened for their ErbB4 expression levels by immunoprecipitation and Western blotting as described below. The clone b1.amg has been described previously (Zhang *et al*., 1996).

Immunoprecipitation and Western blot analysis of ErbB4 levels

To screen for ErbB4 expression levels, individual ErbB4 transfected clones were grown to confluence, lysed and immunoprecipitated with a 1 : 150 dilution of a mouse monoclonal antibody that recognizes an epitope within the extracellular domain of human ErbB4 (clone H4.77.16; Neomarkers) as described previously (Elenius *et al*., 1997b). The immunoprecipitates were separated on 6% SDS–PAGE gels and transferred to 0.1 μm nitrocellulose membranes (Schleicher and Schuell Inc.). The filters were incubated in the presence of a 1 : 50 dilution of a rabbit polyclonal antibody raised against a peptide corresponding to a sequence in the cytoplasmic domain of human ErbB4 (C-18; Santa Cruz Biotechnology, Inc.) and the bound antibody was visualized using a peroxidase conjugated anti-rabbit IgG secondary antibody (1 : 10 000 dilution; Jackson Immunoresearch Laboratories, Inc.) combined with enhanced chemiluminescence (ECL; Amersham).

Tyrosine phosphorylation and coprecipitation analysis

Tyrosine phosphorylation and coprecipitation in response to growth factor stimulation was analysed in confluent cultures of NIH3T3 clone seven transfectants. Cells starved without serum for 24 h were incubated with or without 100 ng/ml of NRG-1 in DMEM and the levels of ErbB4-specific tyrosine phosphorylation were measured by immunoprecipitation with the monoclonal anti-ErbB4 antibody followed by Western blotting using 4G10 antiphosphotyrosine antibody (a kind gift from Dr B Drucker, Dana Farber Cancer Institute, Boston, MA, USA), peroxidase conjugated anti-mouse IgG secondary antibody (1 : 10 000 dilution; Cappel) and ECL. The PI3-K-associated tyrosine phosphorylation was measured by immunoprecipitation with a monoclonal antibody against the p85 subunit of PI3-K (UBI) followed by Western blotting with 4G10. Co-precipitation of ErbB4 and PI3-K was analysed by immunoprecipitation with the anti-p85 antibody followed by Western blotting with the polyclonal anti-ErbB4 as described. Recombinant human NRG-1 (residues 177–241) corresponding to the EGF-like domain of heregulin-β1) was kindly provided by Dr M Sliwkowski (Genetech, Inc., South San Francisco, CA, USA).

Radio-iodination and cross-linking

NRG-1 was radio-iodinated using IODO-BEADS (Pierce) as described (Elenius *et al*., 1997b). A specific activity of 117 000 c.p.m./ng was achieved. For cross-linking of ^{125}I-NRG-1 to cell surface receptors, cells were plated on 20 cm^2 dishes and grown to confluency. Cells were cross-linked with 200 μM disuccinimidyl suberate (DSS; Pierce) in the presence of 15–30 ng/ml of ^{125}I-NRG-1 and the cross-linked complexes were visualized by 6% SDS–PAGE and autoradiography (Elenius *et al*., 1997b).

PI3-K in vitro *kinase assay*

For PI3-K *in vitro* kinase assays, NIH3T3 transfectants were grown to confluence in 175 cm^2 dishes, starved without serum for 24 h, stimulated with or without 100 ng/ml NRG-1 and lysed. The lysates were then immunoprecipitated with polyclonal anti-ErbB4, monoclonal antiphosphotyrosine (4G10) or monoclonal anti-p85 antibodies as described (Elenius *et al*., 1997b). An *in vitro* kinase assay for PI3-K was used to measure PI3-K activity in the immunoprecipitates as previously described (Whiteman *et al*., 1985; Auger *et al*., 1989). Briefly, the phosphorylation of phosphatidyl inositol (PI; Avanti Polar Lipids) with [γ-^{32}P]ATP (DuPont) to form PI^{32}P was analysed using thin-layer chromatography (TLC) and PI^{32}P was visualized by autoradiography and quantitated with densitometry.

Acknowledgements
The authors want to thank Dr Gerhard Raab for valuable discussions of the project and Pia Kuivas for excellent technical assistance. This work was supported by the Academy of Finland (KE), the Ernst Schering Research Foundation (KE and EN), the Harvard Medical School Office of Enrichment Research Fellowship (CJC), the American Heart Association (SP), the Angiogenesis Foundation (SP), the Karin Grunebaum Foundation (SP), and the NIH grants GM 47397 and CA 37392 (MK).

References

Auger KR, Serunian LA, Soltoff SP, Libby P and Cantley LC. (1989). *Cell,* **57,** 167–175.

Bermingham-McDonough O, McCabe KL and Reh TA. (1996). *Development,* **122,** 1427–1438.

Canoll PD, Musacchio JM, Hardy R, Reynolds R, Marchionni MA and Salzer JL. (1996). *Neuron,* **17,** 229–243.

Carpenter G and Wahl MI. (1991). In: *Peptide growth factors and their receptors*. Sporn MB and Roberts AB. (eds). Springer-Verlag: New York, pp. 69–171.

Carraway KL, Weber JL, Unger MJ, Ledesma J, Yu N, Gassmann M and Lai C. (1997). *Nature,* **387,** 512–516.

Chang H, Riese DJ, Gilbert W, Stern DF and McMahan UJ. (1997). *Nature,* **387,** 509–512.
Cohen BD, Green JM, Foy L and Fell HP. (1996). *J. Biol. Chem.,* **271,** 4813–4818.
Culouscou JM, Carlton GW and Aruffo A. (1995). *J. Biol. Chem.,* **270,** 12857–12863.
Dong Z, Brennan A, Liu N, Yarden Y, Lefkowitz G, Mirsky R and Jessen KR. (1995). *Neuron,* **15,** 585–596.
Elenius K, Corfas G, Paul S, Choi CJ, Rio C, Plowman GD and Klagsbrun M. (1997a). *J. Biol. Chem.,* **272,** 26761–26768.
Elenius K, Paul S, Allison G, Sun J and Klagsbrun M. (1997b). *EMBO J.,* **16,** 1268–1278.
Falls DL, Rosen KM, Corfas G, Lane WS and Fischbach GD. (1993). *Cell,* **72,** 801–815.
Franke TF, Kaplan DR and Cantley LC. (1997). *Cell,* **88,** 435–437.
Gassmann M, Casagranda F, Orioli D, Simon H, Lai C, Klein R and Lemke G. (1995). *Nature,* **378,** 390–394.
Gilbertson RJ, Perry RH, Kelly PJ, Pearson ADJ and Lunec J. (1997). *Cancer Res.,* **57,** 3272–3280.
Higashiyama S, Abraham JA, Miller J, Fiddes JC and Klagsbrun M. (1991). *Science,* **251,** 936–939.
Higashiyama S, Horikawa M, Yamada K, Ichino N, Nakano N, Nakagawa T, Miyagawa J, Matsushita N, Nagatsu T, Taniguchi N and Ishiguro H. (1997). *J. Biochem. (Tokyo),* **122,** 675–680.
Holgado-Madruga M, Emlet DR, Moscatello DK, Godwin AK and Wong AJ. (1996). *Nature,* **379,** 560–564.
Holmes WE, Sliwkowski MX, Akita RW, Henzel WJ, Lee J, Park JW, Yansura D, Abadi N, Raab H, Lewis GD, Shepard HM, Kuang W-J, Wood WI, Goeddel DV and Vandlen RL. (1992). *Science,* **256,** 1205–1210.
Hynes NE and Stern DF. (1994). *Biochim. Biophys. Acta,* **1198,** 165–184.
Karunagaran D, Tzahar E, Beerli RR, Chen X, Graus-Porta D, Ratzkin BJ, Seger R, Hynes NE and Yarden Y. (1996). *EMBO J.,* **15,** 254–264.
Komurasaki T, Toyoda H, Uchida D and Morimoto S. (1997). *Oncogene,* **15,** 2841–2848.
Kraus MH, Issing W, Miki T, Popescu NC and Aaronson SA. (1989). *Proc. Natl. Acad. Sci. USA,* **86,** 9193–9197.
Lee K-F, Simon H, Chen H, Bates B, Hung M-C and Hauser C. (1995). *Nature,* **378,** 386–389.
Levkowitz G, Klapper LN, Tzahar E, Freywald A, Sela M and Yarden Y. (1996). *Oncogene,* **12,** 1117–1125.
Marchionni MA, Goodearl ADJ, Chen MS, Bermingham-McDonogh O, Kirk C, Hendricks M, Danehy F, Misumi D, Sudhalter J, Kobayashi K, Wroblewski D, Lynch C, Baldassare M, Hiles I, Davis JB, Hsuan JJ, Totty NF, Otsu M, McBurney RN, Waterfield MD, Stroobant P and Gwynne D. (1993). *Nature,* **362,** 312–318.
Miettinen PJ, Berger JE, Meneses J, Phung Y, Pedersen RA, Werb Z and Derynck R. (1995). *Nature,* **376,** 337–341.
Moscoso LM, Chu GC, Gautam M, Noakes PG, Merlie JP and Sanes JR. (1995). *Dev. Biol.,* **172,** 158–169.
Pinkas-Kramarski R, Eilam R, Spiegler O, Lavi S, Liu N, Chang D, Wen D, Schwartz M and Yarden Y. (1994). *Proc. Natl. Acad. Sci. USA,* **91,** 9387–9391.
Plowman GD, Culouscou JM, Whitney GS, Green JM, Carlton GW, Foy L, Neubauer MG and Shoyab M. (1993). *Proc. Natl. Acad. Sci. USA,* **90,** 1746–1750.
Riese DJ, Bermingham Y, van Raaij TM, Buckley S, Plowman GD and Stern DF. (1996). *Oncogene,* **12,** 345–353.
Riethmacher D, Sonnenberg-Riethmacher E, Brinkman V, Yamaai T, Lewin GR and Birchmeier C. (1997). *Nature,* **389,** 725–730.
Sawyer C, Hiles I, Page M, Crompton M and Dean C. (1998). *Oncogene,* **17,** 919–924.
Schlessinger J and Ullrich A. (1992). *Neuron,* **9,** 383–391.
Shing Y, Christofori G, Hanahan D, Ono Y, Sasada R, Igarashi K and Folkman J. (1993). *Science,* **259,** 1604–1607.
Shoyab M, Plowman GD, McDonald VL, Bradley JG and Todaro GJ. (1989). *Science,* **243,** 1074–1076.
Sibilia M, Steinbach JP, Stingl L, Aguzzi A and Wagner EF. (1998). *EMBO J.,* **17,** 719–731.
Sibilia M and Wagner EF. (1995). *Science,* **269,** 234–238.
Soltoff SP and Cantley LC. (1996). *J. Biol. Chem.,* **271,** 563–567.
Soltoff SP, Carraway KLR, Prigent SA, Gullick WG and Cantley LC. (1994). *Mol. Cell. Biol.,* **14,** 3550–3558.
Songyang Z, Shoelson SE, Chaudhuri M, Gish G, Pawson T, Haser WG, King F, Roberts T, Ratnofsky S, Lechleider RJ, Neel BG, Fajardo JE, Chou MM, Hanafusa H, Schaffhausen B and Cantley C. (1993). *Cell,* **72,** 767–778.
Threadgill DW, Dlugosz AA, Hansen LA, Tennenbaum T, Lichti U, Yee D, LaMantia C, Mourton T, Herrup K, Harris RC, Barnard JA, Yuspa SH, Coffey RJ and Magnuson T. (1995). *Science,* **269,** 230–234.
Toker A and Cantley LC. (1997). *Nature,* **387,** 673–676.
Tokunaga K, Taniguchi Y, Yoda K, Shimizu M and Sakiyama S. (1986). *Nucleic Acids Res.,* **14,** 2829.
Toyoda H, Komurasaki T, Uchida D, Takayama Y, Isobe T, Okuyama T and Hanada K. (1995). *J. Biol. Chem.,* **270,** 7495–7500.
Ullrich A, Coussens L, Hayflick JS, Dull TJ, Gray A, Tam AW, Lee J, Yarden Y, Libermann TA, Schlessinger J, Downward J, Mayes ELV, Whittle N, Waterfield MD and Seeburg PH. (1984). *Nature,* **309,** 418–425.
Wada T, Qian XL and Greene MI. (1990). *Cell,* **61,** 1339–1347.
Wen D, Peles E, Cupples R, Suggs SV, Bascus SS, Luo Y, Trail G, Hu S, Silbiger SM, Levy RB, Koski RA, Lu HS and Yarden Y. (1992). *Cell,* **69,** 559–572.
Whitman M, Kaplan DR, Schaffhausen B, Cantley L and Roberts TM. (1985). *Nature,* **315,** 239–242.
Yamamoto T, Ikawa S, Akiyama T, Semba K, Nomura N, Miyajima N, Saito T and Toyoshima K. (1986). *Nature,* **319,** 230–234.
Yao R and Cooper GM. (1995). *Science,* **267,** 2003–2006.
Zhang D, Sliwkowski MX, Mark M, Frantz G, Akita R, Sun Y, Hillan K, Crowley C, Brush J and Godowski PJ. (1997). *Proc. Natl. Acad. Sci. USA,* **94,** 9562–9567.
Zhang K, Sun J, Liu N, Wen D, Chang D, Thomason A and Yoshinaga SK. (1996). *J. Biol. Chem.,* **271,** 3884–3890.
Zhao Y-Y, Sawyer DR, Baliga RR, Opel DJ, Han X, Marchionni MA and Kelly RA. (1998). *J. Biol. Chem.,* **273,** 10261–10269.
Zimonjic DB, Alimandi M, Miki T, Popescu NC and Kraus MH. (1995). *Oncogene,* **10,** 1235–1237.